Low temperature dynamics of H + HeH+→ H2+ + He reaction: On the importance of long-range interaction

Jayakrushna Sahoo, Duncan Bossion, Tomás González-Lezana, Dahbia Talbi, Yohann Scribano

Low temperature dynamics of H + $HeH^+ \rightarrow H_2^+$ + He reaction: On the importance of long-range interaction

Jayakrushna Sahoo,[1, a)] Duncan Bossion,[2] Tomás González-Lezana,[3] Dahbia Talbi,[1] and Yohann Scribano[1, b)]

[1)]*Laboratoire Univers et Particules de Montpellier, Université de Montpellier, UMR-CNRS 5299, 34095 Montpellier Cedex, France*

[2)]*IPR - Université de Rennes Bât 11b, Campus de Beaulieu, 263 avenue du Général Leclerc 35042 Rennes Cedex, France*

[3)]*Instituto de Física Fundamental, IFF-C.S.I.C., Serrano 123, Madrid 28006, Spain*

While the growing realization of the importance of long-range interactions is being demonstrated in cold and ultracold bimolecular collision experiments, their influence on one of the most critical ion-neutral reactions has been overlooked. Here, we address the non-Langevin abrupt decrease observed earlier in the low energy integral cross sections and rate coefficients of the astrochemically important H + $HeH^+ \rightarrow H_2^+$ + He reaction. We attribute this to the presence of artificial barriers on existing potential energy surfaces (PESs). By incorporating precise long-range interaction terms, we introduce a new refined barrierless PES for the electronic ground state of HeH_2^+ reactive system, aligning closely with high level *ab initio* electronic energies. Our findings, supported by various classical, quantum, and statistical methods, underscore the significance of long-range terms in accurately modeling reactive PESs. The low temperature rate coefficient on this new PES shows a substantial enhancement as compared to the previous results and aligns with Langevin behavior. This enhancement could affect noticeably the impact HeH^+ abundance prediction in early Universe condition.

[a)]Electronic mail: jayakrushna.sahoo@umontpellier.fr

[b)]Electronic mail: yohann.scribano@umontpellier.fr

I. INTRODUCTION

Recent progress in gas-phase bimolecular collisions has demonstrated the importance of complementarity between experimental measurements and theoretical calculations in molecular reaction dynamics to a great extent.[1–4] The potential energy surface (PES) serves as the bridge between theory and experiment both in gas phase and condensed phase molecular dynamics.[5,6] It describes the total energy relative to a specific electronic state of the molecular system, as a function of the nuclear coordinates of each atom involved.[5,6] The credibility of theoretical predictions depends on the accuracy of the PES, which must reliably replicate experimental data within uncertainties, assuming the dynamical calculation method is sufficiently accurate. For reactions involving transition states, an accurate description of the location and energetic height of the barrier along the reaction path is crucial in predicting dynamical outcomes.[7,8] On the other hand, for exoergic and barrierless reactions, an accurate description of the long-range interaction potential becomes mandatory.[8–10]

Exoergic-barrierless reactions are key processes in diverse fields, such as early Universe chemistry,[11,12] interstellar gas clouds,[13,14] planetary and stellar atmospheres,[15] combustion processes, and fusion plasma.[16,17] Their barrierless nature leads to high rate coefficients even at low temperatures, showing non-Arrhenius behavior.[8,9] The long-range attractive interactions result in significant reactive and inelastic scattering cross-sections, particularly at low collision energies.[6] These reactions often follow the Wigner threshold laws[18,19] at ultracold temperatures and can be described by the classical Langevin capture model at thermal energies.[20–22] They frequently involve complex formation, making them suitable for description by statistical models[23–27] combined with simple capture approximations.[28–30]

Over the past decade, rapid advancements in experimental techniques for cooling a molecule's translational as well as internal energy down to a few Kelvin have enabled the study of molecular collisions at cold and ultracold temperature conditions.[31–34] Additionally, techniques like the merged beam approach with Rydberg molecules/atoms allow to investigate ion-neutral reactions effectively even at a few milliKelvin.[31,32,35–37] These low-temperature investigations effectively probe the long-range part of the PES[38–40] and have succeeded in testing theoretical predictions based on capture theories relevant to various types of long-range interactions arising from ion-dipole and ion-multipole interactions.[41–49] Such studies not only demonstrated the effect of the anisotropy of the long-range potential in explaining the large deviation of low-temperature rate

coefficients from the classical Langevin model[42–44,46,50] but also experimentally verified the phenomenon of "quantum capture"[51,52] of molecules with no dipole or quadrupole moments by ions.

As a consequence of the unequivocal success of these investigations, there is a growing consensus that long-range interactions play a major role in ion-neutral reactions at low and ultra-low energies and must be taken into account in any theoretical simulation pertaining to such type of reactions.[10,53,54] Although there have been numerous studies of exoergic-barrierless bimolecular reactions at cold and ultracold temperature conditions,[21,33,34,55] low-temperature studies with proper treatment of long-range interactions for one of the important ion-neutral reactions have been overlooked. This reaction, the focus of the present work, involves the destruction of the HeH^+ cation by the H atom to form H_2^+ and He:

$$H + HeH^+ \rightarrow H_2^+ + He \qquad \text{(R1)}.$$

The above reaction holds a considerable importance in astrochemistry, particularly in helium and hydrogen reaction networks,[11] and is one of the essential process for the formation of primordial H_2 from H_2^+ ions.[11,12,56]

The HeH^+ ion is believed to be the first molecular species to have appeared in the early Universe[57,58] after the Big Bang Nucleosynthesis and is thought to have initiated the chemistry of the Universe via reaction (R1).[11,12,58,59] The detection of interstellar HeH^+ ion was only recently achieved[60–62] by direct observation of its rovibrational emission lines from the planetary nebula NGC 7027, after numerous unsuccessful attempts in the past.[63–67] The discrepancy between the observed line strength and theoretical model prediction[60,62] has renewed interest in studying the role of HeH^+ in cosmic chemistry[68–73] and its potential implications for our understanding of early astrophysical environments.[68,74–77]

The reaction (R1) is barrierless and exoergic by ≈ 0.75 eV. The PES of HeH_2^+ system possesses a deep potential well corresponding to the collinear ionic complex $[He\cdots H\cdots H]^+$ which lies $\approx$ 1.087 eV below the bottom of $H + HeH^+$ valley.[78] Additionally, it exhibits another shallow well corresponding to the collinear complex $[H\cdots He\cdots H]^+$ which lies just ≈ 0.067 eV below the bottom of $H + HeH^+$ valley[78] (see section 1 of the supplementary material for more details on the topography of HeH_2^+ PES).

Available experimental measurements for reaction (R1) are those performed in the seventies by Karpas *et al.*[79] and Rutherford and Vroom[80] using ion cyclotron resonance and crossed ion

neutral beam techniques, respectively. In the last decade, several theoretical calculations have been carried out by using both classical and quantum mechanical methods to predict the cross section, rate coefficient and product rotational angular momentum polarization of reaction (R1).[81–89] The PES used in all of these studies is that developed by Ramachandran *et al.*[78] This PES was generated by calculating the *ab initio* electronic energies using both multi-reference[90,91] and full configuration interaction[92,93] (MRCI and FCI) methods with correlation consistent polarized valence quadruple- and quintuple-zeta[94] (cc-pVQZ and cc-pV5Z) basis sets, and then analytically fitting them afterwards by Aguado-Paniagua functions[95] with the polynomials of highest order M = 6 and 8. Consequently, three PES subroutines were reported by Ramachandran *et al.*[78]; M=6 fit of MRCI/cc-pV5Z (hereafter RMRCI6), M=8 fit of MRCI/cc-pV5Z (hereafter RMRCI8) and M=8 fit of FCI/cc-pVQZ energy points (hereafter RFCI8). The root mean square error (RMSE) of the above PESs were reported as 14, 7 and 6 meV, respectively. Koner *et al.*[96] recently reported a new non-reactive PES of the H_2^+–He system where the the *ab initio* electronic energies were calculated at both MRCI with Davidson correction (MRCI+Q)[90] and FCI levels of theory with aug-cc-pV6Z[97] and aug-cc-pV5Z[98] basis sets, respectively. Accurate long-range interactions extending up to R^{-8} term (R being the internulcear separation) were included analytically with smooth scaling and switching functions.[96] The RMSEs of the MRCI+Q and FCI PESs were reported to as 2.16 cm^{-1} (~0.26 meV) and 0.92 cm^{-1} (~0.11 meV), respectively. This PES was constructed only for the H_2^+–He interaction and does not extend to the asymptote of H + HeH^+ channel. Hence, it is not suitable for reactive dynamics study.

Although the reaction observable data obtained from PESs of Ramachandran *et al.*[78] were later used in astrochemical predictions,[76,77,83] the behavior of the cross section and rate coefficient of reaction (R1) calculated on these PESs is highly questionable. This is because in all of the above theoretical investigations, the integral cross section (ICS) was found to abruptly decrease below 10 meV of collision energy for which no explanation was given.[83–89] This behavior of the cross section consequently resulted an unexpected reduction of the rate coefficient at lower temperature range,[83,86,88,89] a range highly relevant for early Universe chemistry at low redshifts.[11,12] This non-Langevin behavior of the ICS and rate coefficient is certainly in contrast with the usual characteristics of an exoergic-barrierless reaction dominated by ion-induced dipole interaction.[6,8,9] It is the purpose of the present work to search for the origin of this problematic behavior and provide a possible remedy for it.

In what follows next, we show in detail that this abrupt decrease in ICS at low energies is

attributable to a so-called "artificial barrier" present on the reaction path of RMRCI6, RMRCI8 and RFCI8 PESs. Furthermore, we show how a correct long-range interaction term can be used to remove this "spurious feature", thus presenting a new "refined" barrierless global PES of the HeH_2^+ reactive system. Employing the new barrierless PES, we calculated the ICS and rate coefficient of reaction (R1) by means of different quasi-classical 5QCT), statistical (SQM) and quantum mechanical (QM) methods. We show that the behavior of our new reaction observables is in accordance with the usual characteristic of an exoergic-barrierless ion-neutral reaction. The rest of the article is organized as follows. The importance of correct long-range interaction in eliminating the "artificial" barrier and the details of construction of a new barrierless PES is described in Sec. II. The dynamical methodology followed in the present investigation is described briefly in Sec. III. The results from the dynamical calculations are discussed in Sec. IV. Finally, a summary of the work and the conclusions are presented in Sec. V.

II. TOWARDS AN ACCURATE GLOBAL BARRIERLESS PES

A. On the importance of long range interaction

While analyzing the topographical details of the PESs of Ramachandran *et al.*, it is found that there exists a barrier to the reaction (R1) near the long-range region from the H + HeH^+ channel. This can readily be seen from Fig. 1 where the minimum energy paths (MEPs) corresponding to collinear approach are plotted for the RMRCI6, RMRCI8 and RFCI8 PESs. The long-range region from the H + HeH^+ channel has been enlarged in the inset for a clear view. This barrier at a first glance seems artificial in nature. This is because the height of the barrier in case of RMRCI6 and RMRCI8 fits of the PES is different and also occur at different nuclear geometry (See section 1 and Fig. S2 of supplementary material) despite the fact that both the fits used same set of *ab initio* energy data in Ref. 78. The height of this artificial barrier along the collinear approach is found to be ~ 4.8, ~ 0.66 and ~ 0.74 meV in case of RMRCI6, RMRCI8 and RFCI8 PESs, respectively. The barrier is also present for other approach angles in non-collinear geometry, however, its height decreases with decreasing $\angle$ HeHH angle from 180 to 0° (See section 1 and Figs. S3 and S4 of supplementary material). It is important to note that the values of barrier-height along the MEPs are less than the RMSE values of the respective PESs. This means the so-called artificial barriers are most likely to be originated from a poor handling of fitting of the *ab initio* energy data. This

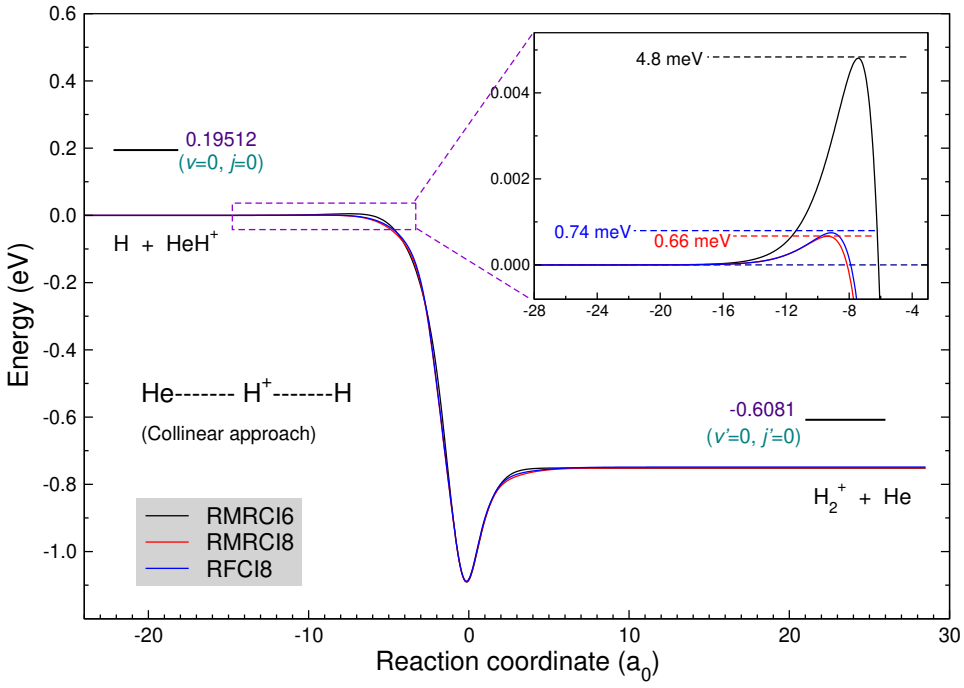

Figure 1: Minimum energy path of reaction R1 at collinear approach i.e., ∠ HeHH = 180°, obtained from RMRCI6, RMRCI8 and FCI8 PESs of Ramachandran *et al.*[78]. The threshold portion of the MEPs from the HeH^+ + H channel is enlarged in the inset to highlight the presence of artificial barrier. The bottom of HeH^+ diatom well is taken as zero of energy.

can have serious implications in the low energy H + HeH^+ collisional dynamics when done using the PESs of Ramachandran *et al.*[78] In particular, the presence of this "artificial" barrier leads to a large reduction in the cross section and rate coefficient in the region of low energy and temperature, respectivley, as already seen in Refs. 83,86–89. The barrier also exists for the approach of H atom towards HeH^+ from the He-side in cases of all three PESs described above (see Fig. S5).

The impact of the artificial barrier on the dynamics is investigated through quasi-classical trajectory (QCT) (See section 3C below for details of the method) simulations. If barriers are truly present on these PESs then the energy dependent profile of the ICS calculated by QCT method will show a clear threshold at an energy close to the barrier-height. This is because the classical trajectories can not tunnel through the barrier and can only surpass it if they have higher energy. The QCT ICS computed on the RMRCI6 and RMRCI8 PESs are shown in Fig. 2. It can be seen from the figure that the QCT ICSs show clear thresholds at lower energies confirming the presence of "artificial" barrier on the PESs of Ramachandran *et al.*[78] Moreover, the threshold of ICS calculated on RMRCI8 PES occurs towards lower energy than that of RMRCI6 PES, which is consistent with the fact that the barrier-height in case of RMRCI8 PES is lower than that in RMRCI6 PES.

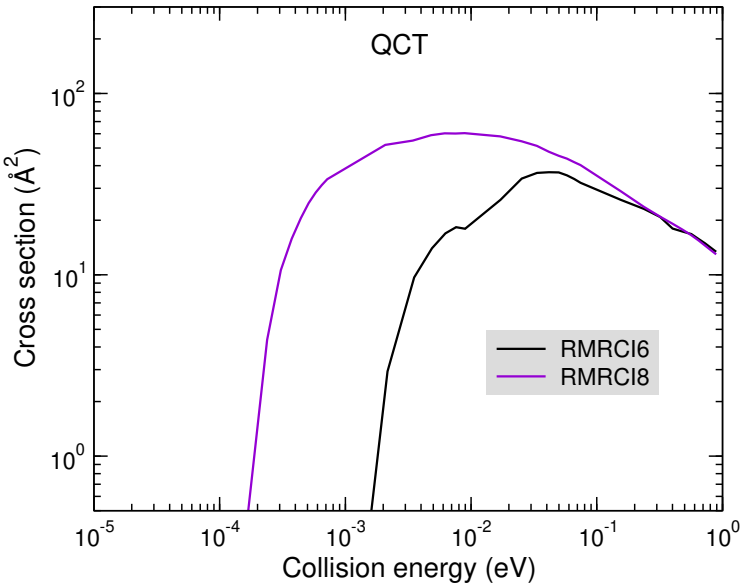

Figure 2: Initial state-selected total ICS of reaction R1 for HeH^+ (v=0, j=0) as a function of collision energy computed with QCT-HB method obtained from RMRCI6 and RMRCI8 PESs of Ramachandran *et al.*[78]

B. Correcting the long range behavior

The PES of reactive molecular system is generally expressed in terms of a many body expansion as it is done for the HeH_2^+ system in Refs. 78,96. For a tri-atomic (A + BC) reactive system, this can be written as,

$$V(r_{AB}, r_{BC}, r_{AC}) = \sum_i V_i^{(1)} + \sum_{i \neq j} V_{ij}^{(2)}(r_{ij}) + V_{ABC}^{(3)}(r_{AB}, r_{BC}, r_{AC}), \quad (1)$$

where $V_i^{(1)}$, $V_{ij}^{(2)}$ and $V_{ABC}^{(3)}$ are the mono-atomic, two-body and three-body terms, respectively, with r_{ij} (i, j=A, B and C) representing the internuclear distances. The two-body pair-wise terms (second summation should count each pair only once) are responsible for the attractive nature of the PES and make a key contribution around the long-range region while the three-body terms are generally repulsive in nature. Since the long-range nature of the two-body potentials mainly affects the this particular region of the PESs, the two-body terms can be efficiently tuned, as it is done in the present case, to effectively remove the "artificial" barrier. It is found that making the two-body terms appropriately attractive by incorporating the correct analytical long-range interaction terms efficiently removes the "artificial" barrier.

The long-range interaction terms added to the two-body potentials in the present work has the

following form.[96,99]

$$V_{\text{long}}(r) = -\frac{\alpha_{\text{d}} q^2}{2r^4} - \frac{\alpha_{\text{q}} q^2}{2r^6} - \frac{\alpha_{\text{o}} q^2}{2r^8} - \frac{\beta_{\text{ddq}} q^3}{6r^7} - \frac{\gamma_{\text{d}} q^4}{24r^8}, \tag{2}$$

where r is the internuclear distance of the diatomic molecule, q is the charge, and α_{d}, α_{q} and α_{o} are the dipole, quadrupole and octopole polarizabilities of H and He, respectively.[99,100] β_{ddq} and γ_{d} are the first and second hyperpolarizabilities, respectively.[99,100]

We first show the importance of two-body long-range terms towards the contributions of overall two- and three-body potentials to the PES. For this purpose the one-dimensional cuts of sum of the three-body and one of the two-body potentials are plotted in Fig. 3 for various combinations of the potentials. Importantly, the three-body term is taken from the RMRCI6, RMRCI8 and RFCI8

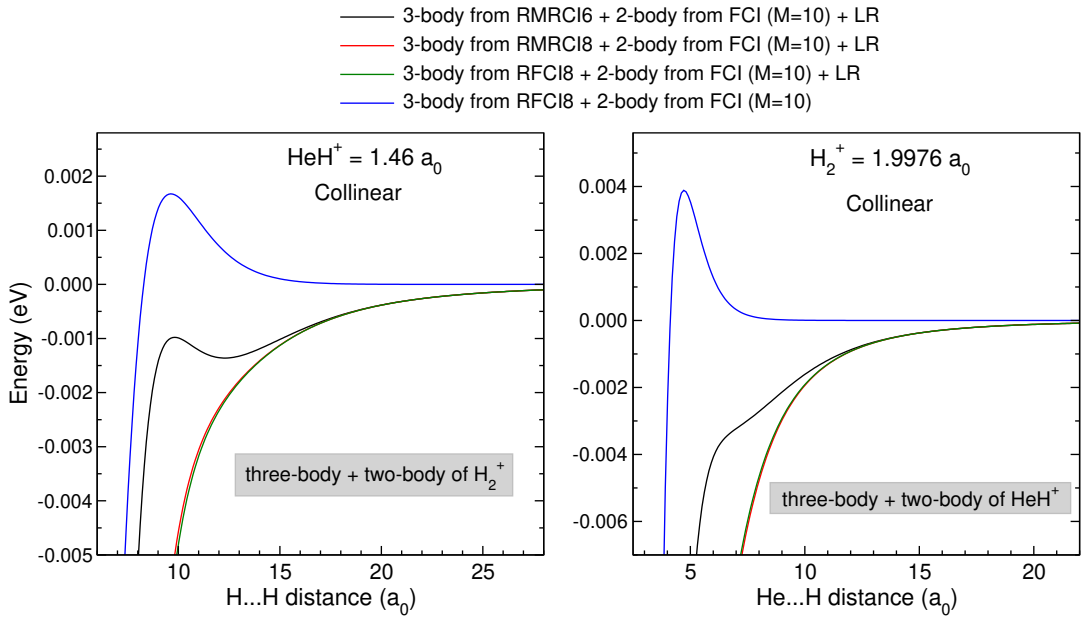

Figure 3: Long-range region of the one-dimensional cuts of three-body plus one of the two-body potentials of various combinations (see text for details) to show the effect of long-range term in removing the artificial barrier. **Left:** three-body plus two-body of H_2^+ at a collinear approach of attacking H towards the H-side of HeH^+, where HeH^+ is fixed at its equilibrium distance. The zero of energy is the bottom of HeH^+ diatom well. **Right:** Same as in left but two-body of HeH^+ is taken at a collinear approach of He towards H_2^+ and H_2^+ is fixed at its equilibrium distance. The zero of energy is the bottom of H_2^+ diatom well.

PESs of Ramachandran *et al.*[78], and the two-body terms are taken from the FCI/aug-cc-pV5Z (M = 10) PES of Koner *et al.*[96] both with and without the long-range. The left panel of Fig. 3 shows the three-body plus H_2^+ two-body potential plotted against H...H distance for a collinear approach of the attacking H atom towards the H-side of HeH^+ fixed at its equilibrium distance. Similarly, the

right panel shows the three-body plus HeH^+ two-body potential as a function of He...H distance for a collinear approach of He towards H_2^+ fixed at its equilibrium distance.

A few observations can be made from Fig. 3. First, it can be seen from both the panels that when the two-body potentials with the improved long-range term are added to the three-body potential, the artificial barrier disappears completely, except for the three-body term from RMRCI6 fit (black solid curve). In case of the latter, an artificial sub-merged barrier and a local minimum remain even with the addition of the two-body potential with accurate long-range terms. Second, even from the same *ab initio* points when the three-body term from RMRCI8 fit is used, the barrier disappears and the resultant one-dimensional potential behaves smoothly near the long-range region (red solid curve), and agrees quite well with the one-dimensional cut where the three-body term is taken from the RFCI8 fit (green solid curve). This suggests that the three-body term, and consequently the full PES, of the RMRCI6 fit of Ramachandran *et al.*[78] is not quite accurate and hence not suitable for dynamical calculations. The inaccuracy mainly lies in the fitting of the three-body as well as the two-body potentials, which results in an artificial barrier. Third, even with the improved M = 8 fit of the three-body term and M = 10 fit of the two-body term but without the long-range (from Ref. 96), the resultant one-dimensional cut exhibits the artificial barrier (blue solid line). This demonstrates the importance of the two-body long-range terms in determining smooth topography of the underlying PES.

Hence, with the use of accurate and improved two-body long-range terms, the artificial barrier present in the PESs of Ramachandran *et al.*[78] can be completely removed, provided an accurate three-body fit must be employed. In the present work, a new "refined" and barrierless PES is constructed by adding the FCI/aug-cc-pV5Z (M = 10) two-body terms with long-range interactions from Ref. 96 to the RFCI8 three-body term of Ref. 78. Although, the *ab initio* points of RFCI8 PES in Ref. 78 were obtained by a lower level of basis sets as compared to that in Ref. 96, we note here that the RFCI8 three-body term of Ref. 78 is the only accurate three-body fit available till date that can be used to construct a global reactive PES for the HeH_2^+ system. The readers are referred to section 2 of supplementary material for details about the construction of the new "refined" PES.

In order to check the correct topography of the new refined PES, one-dimensional cut corresponding to the restricted geometry same as in left panel of Fig. 3 is presented in Fig. 4 along with those obtained from the RMRCI6, RMRCI8 and RFCI8 PESs for a comparison. To clarify further, *ab initio* electronic energies corresponding to the same geometries are calculated in the present work by MRCI+Q method[90] with aug-cc-pV6Z[97] basis set. The reference wave func-

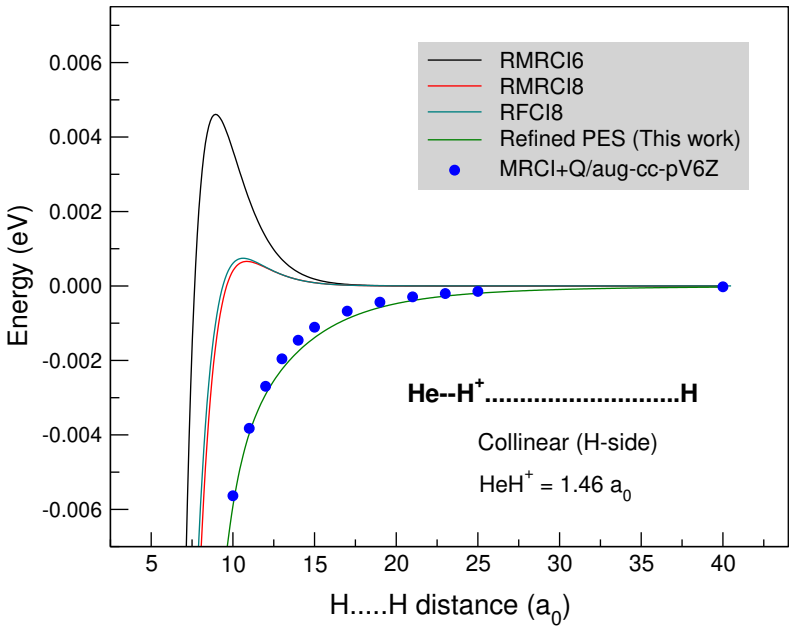

Figure 4: Comparison of the one-dimensional cuts of the new "refined" PES with the *ab initio* energies calculated in the present work and those obtained from RMRCI6 and RMRCI8 PESs of Ramachandran *et al.*[78] highlighting the removal of the "artificial" barrier. The zero of energy is the bottom of HeH^+ diatom well.

tions for MRCI calculation were obtained using the complete active space self-consistent field (CASSCF)[101,102] method with an active space of a total of fifteen orbitals; three 1s, three 2s and nine 2p orbitals for H and He. The electronic structure calculations were carried out with the Molpro quantum chemistry package.[103] The MRCI+Q/aug-ccpV6Z energies are shown in Fig. 4 for a rigorous comparison. It is clear from Fig. 4 that there are no artificial barriers present in the new "refined" PES nor in the *ab initio* energies, unlike in the case of RMRCI6, RMRCI8 and RFCI8 PESs of Ramachandran *et al.*[78] Moreover, the topography of our "refined" PES closely agrees with the *ab initio* initio energies in the long-range region indicating the high accuracy of our "refined" PES. A comparative account of a few more one-dimensional cuts of the PESs at different geometries and the MEPs are shown in Figs. S6 and S7.

III. DYNAMICAL METHODS

The dynamics of reaction R1 is investigated by three different methodologies each based on different theoretical foundations; namely, time-independent quantum mechanical (TIQM) method, statistical quantum method (SQM) and quasi-classical trajectory (QCT) methods. The details of these methods are given below. A brief description of the Langevin model that used in the present

work is given at the end of this section.

A. Quantum reactive scattering

The quantum scattering dynamics of reaction R1 is carried out here by means of TIQM method as implemented in the ABC program of Manolopoulos and co-workers.[104] The ABC code uses a coupled-channel hyperspherical coordinate method to solve the time-independent Schrödinger equation for the nuclear motion of a triatomic reactive system. In the ABC program the set of coupled-channel hyperradial equations are solved by log-derivative method[105] and the scattering matrix (S-matrix) is obtained by applying asymptotic boundary conditions at large value of hyperradius. On a single run of the code, the S-matrix elements are obtained in a specified energy range for a specific value of total angular quantum number J and the triatomic parity eigenvalue P for all the three reactive channels. In the present case the value of diatomic parity is set as 0 since the reactant diatom HeH^+ is hetero-nuclear. Various reaction observables like reaction probability, ICS and rate constant are calculated from the S-matrix elements. The reaction probabilities are obtained by taking the modulus square of the S-matrix elements in helicity representation. The helicity-representation S-matrix elements $S^J_{vj\Omega\rightarrow v'j'\Omega'}(E)$ are obtained by appropriately combining the parity adapted S-matrix elements as given in Eq. (1) and (2) of ref. 104. The symbols v, j and Ω denote the vibrational, rotational and helicity quantum numbers of the reactant channel, and the corresponding prime quantities denote the same for the product channel. The initial rovibrational state-selected ICS is calculated as

$$\sigma_{vj}(E) = \frac{\pi}{\tilde{k}^2_{vj}} \frac{1}{2j+1} \sum_{v'j'} \sum_{J=0}^{J_{\max}} \sum_{\Omega\Omega'} g_{j'}(2J+1) \left| S^J_{vj\Omega\rightarrow v'j'\Omega'}(E) \right|^2. \tag{3}$$

Here, $\tilde{k}_{vj} = \sqrt{2\mu E_{\rm col}}/\hbar$, with μ being the atom-diatom reduced mass of the reactant channel, $E_{\rm col}$ is the collision energy which is the total energy (E) minus the rovibrational energy of the reactant diatom. The quantity $g_{j'}$ is the post-antisymmetrization factor[106,107] which takes into account the effect of nuclear spin upon exchange of two identical nuclei in the diatomic product molecule. It takes the value of 3/2 (1/2) corresponding to odd (even) j' quantum number of H_2^+ diatom.[106,107]

The initial state-specific temperature dependent rate coefficients are calculated from the corre-

sponding ICSs (σ_{vj}) by thermal averaging over a Maxwell-Boltzmann velocity distribution as

$$k_{vj}(T) = \sqrt{\frac{8k_BT}{\pi\mu}}\frac{1}{(k_BT)^2}\int_0^\infty E_{\rm col}\sigma_{vj}(E_{\rm col})e^{-E_{\rm col}/k_BT}\mathrm{d}E_{\rm col} \tag{4}$$

where k_B is the Boltzmann constant. Although the limit of the integration in Eq. 4 is from 0 to ∞, in practice the integration is performed here by a numerical trapezoidal rule from certain values of $\mathrm{E_{col,min}}$ to $\mathrm{E_{col,max}}$.

The thermal rate coefficient at a given temperature is calculated by averaging the initial state-specific rate coefficients over a Boltzmann distribution of initial rovibrational states as

$$k(T) = \frac{1}{Q_{\rm rovib}(T)}\sum_{vj}k_{vj}(T)(2j+1)e^{-\epsilon_{vj}/k_BT} \tag{5}$$

where

$$Q_{\rm rovib}(T) = \sum_{vj}(2j+1)e^{-\epsilon_{vj}/k_BT} \tag{6}$$

is the rovibrational partition function and ϵ_{vj} is the energy of $(v,\ j)$ rovibrational level of HeH^+ ion. The numerical parameters used in the TIQM calculation and details of the convergence analysis are given in Section III of the supplementary material.

B. Statistical quantum method

The SQM reported in Refs. 25–27 has been employed in this work. This approach was specially conceived for atom-diatom reactions which proceed via the formation of an intermediate complex between reactants and products. Within the framework of this method, the state-to-state reaction probability $P^J_{vj,v'j'}(E_{\rm col})$ between the $HeH^+(v,\ j)$ and $H_2^+(v',\ j')$ rovibrational states for a value of the total angular momentum J and collision energy $E_{\rm col}$, can be approximated as:

$$P^J_{v,j;v'j'}(E_{\rm col}) = \left|S^J_{v,j;v'j'}(E_{\rm col})\right|^2 \simeq \frac{p^J_{v,j}(E_{\rm col})p^J_{v'j'}(E_{\rm col})}{\sum_{v''j''}p^J_{v''j''}(E_{\rm col})}, \tag{7}$$

where $p^J_{v,j}(E_{\rm col})$ is the individual capture probability for the formation of the above mentioned collision complex from reactants and $p^J_{v'j'}(E_{\rm col})$ the probability of the complex to fragment onto the corresponding final product state. In Eq. (7) the sum in the denominator runs for all rovibrational

states energetically open in both the reactant and product arrangements. The individual capture probabilities are obtained by means of a time independent method described in Refs. 25,26, which involves a log derivative propagation between the asymptotic region R_{max} and a capture radius R_{min} defined separately for reactants and products. The solution of the corresponding equations is done within a coupled-channel scheme. Values for such R_{min} and R_{max} are the same as in our previous investigation on the title reaction[89]: 1.57 and 36.67 Å, for the H + HeH^+ arrangement, and, 1.28 and 29.0 Å, for the products He + H_2^+.

ICSs are calculated using the state-to-state probability of Eq. (7) in Eq. (3). The resulting values are then employed in Eq. (4) to calculate the rate coefficient.

C. Quasi-classical trajectory calculations

The details of the QCT methodology can be found in previous papers.[108–110] It consists in classical dynamics of the nuclear degrees of freedom on the PES. The internal energy of the initial diatomic (here the HeH^+) in a given rovibrational state (v, j) corresponds exactly to the energy of that state. The attribution of the final rovibrational state is done based on quasi-quantum rotational and vibrational quantum number obtain within the WKB approximation.[111] The calculations done here using the QCT method are similar to what was done in the previous work on the same system by some of the authors,[89] but with the difference that the traditional histogram binning is used here for the attribution of both the final vibrational and rotational quantum numbers from the pseudo-quantum numbers instead of the Gaussian binning. The same parameters and energy values are used for the RMRCI6 and RMRCI8 PESs of Ramachandran *et al.*[78] and for the new "refined" PES. Cross sections are computed with collision energies starting from 5×10^{-5} eV up to 0.7 eV with values every 2.5×10^{-6} Hartree ($\approx 6.8 \times 10^{-5}$ eV) for the low energy domain to obtain a fine energy grid. The initial impact parameter convergence is ensured by taking its values up to 180 a_0 (results where converged over 65 a_0) for the lowest energies. Up to 10^5 trajectories were propagated to minimize the standard deviation of the cross section.

D. Classical Langevin model

Ion-neutral reactions dominated by ion-induced-dipole long-range interaction, where the interaction potential vary with intermolecular distance as $-C_4/R^4$, are often described by Langevin

capture model.[112–114] Such capture model relies on the assumption that the rate of ion-neutral reaction only depend on the long-range electrostatic interactions between charge of the ion and induced polarizability of the neutral species. According to the classical Langevin model[112–114] the reaction cross section (σ_{L}) and rate coefficient (k_{L}) can be obtained as,

$$\sigma_{\mathrm{L}} = 2\pi \sqrt{\frac{C_4}{\mathrm{E_{col}}}} \tag{8}$$

and

$$k_{\mathrm{L}} = 2\pi \sqrt{\frac{2C_4}{\mu}}, \tag{9}$$

respectively, with $C_4 = \frac{1}{2}\frac{q^2\alpha}{(4\pi\epsilon_0)^2}$, where α, q, ϵ_0 and μ are the polarizability of the neutral reactant (H atom in the present case), the charge on the ionic reactant, the permittivity of vacuum and the reduced mass of the collision system. A value of $\alpha = 4.5$ au for the H atom has been used.[100] The characteristic feature of classical Langevin cross section is that it gives a slope of negative one-half when plotted as a function of $\mathrm{E_{col}}$ in the double logarithmic scale. Consequently, it predicts a temperature-independent rate coefficient for ion-neutral reaction dominated by ion-induced-dipole interactions.

IV. RESULTS AND DISCUSSION

The influence of the long-range interaction on the dynamics of reaction (R1) is examined here in terms of the reaction observables calculated by TIQM, SQM and QCT methods. The results obtained from these dynamical methods along with the classical Langevin model results are presented and discussed below.

First, the probability of reaction (R1) obtained from the TIQM calculations using different forms of PES are shown in Fig. 5 for zero total angular momentum (J=0). It is clear from the figure that for collision energies higher than 10 meV, all the probabilities vary closely with each other, whereas for lower collision energies, clear differences persists among them. To understand the impact of the "artificial" barrier, one can compare the reaction probabilities obtained using RMRCI6, RMRCI8 and the newly constructed "refined" PES of the present work at lower collision energy. The probabilities from RMRCI6 and RMRCI8 PESs drops down exponentially towards zero at lower collision energies as a consequence of the barrier, whereas the probability from the

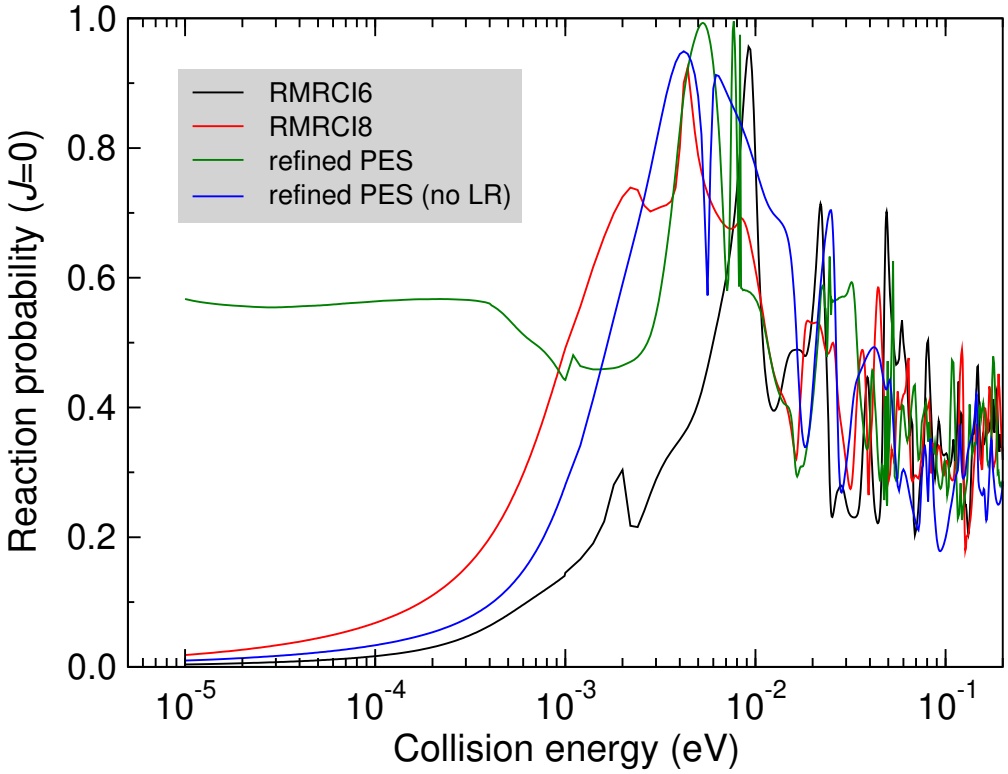

Figure 5: Initial state-selected total reaction probabilities of reaction R1 for HeH^+ (v=0, j=0) and J=0 calculated on the new "refined" PES (both with and without the long-range terms) in the present work compared with those obtained on the RMRCI6 and RMRCI8 PESs of Ramachandran *et al.*[78]. The probabilities are plotted in the semi-log scale (only along the abscissa) to highlight their low energy behavior.

new "refined" PES remains significant (slightly over 0.5) around the same energies. Since QM calculations for J=0 do not involve any additional barriers due to centrifugal terms, it is clear that the new three-dimensional "refined" PES is truly barrierless. The probability is also obtained using a modified PES without the inclusion of two-body long-range terms to examine their effect on the reaction dynamics, and is shown in Fig. 5 with a solid blue line. The reaction probability in this case behaves similarly to the case of RMRCI6 and RMRCI8 suggesting the presence of an "artificial" barrier (similar to RMRCI6 and RMRCI8 PESs) on the modified PES without the long-range terms. This emphasizes the importance of inclusion of correct long-range terms while completely removing the "artificial" barrier.

The ICSs of reaction (R1) calculated by TIQM, SQM and QCT methods using the new "refined" PES are compared with the previous literature results obtained on the RMRCI6 PES in the left panel of Fig. 6. The ICS obtained from the classical Langevin model is also shown for comparison. The most striking feature that can be observed is the difference in the low energy behavior of

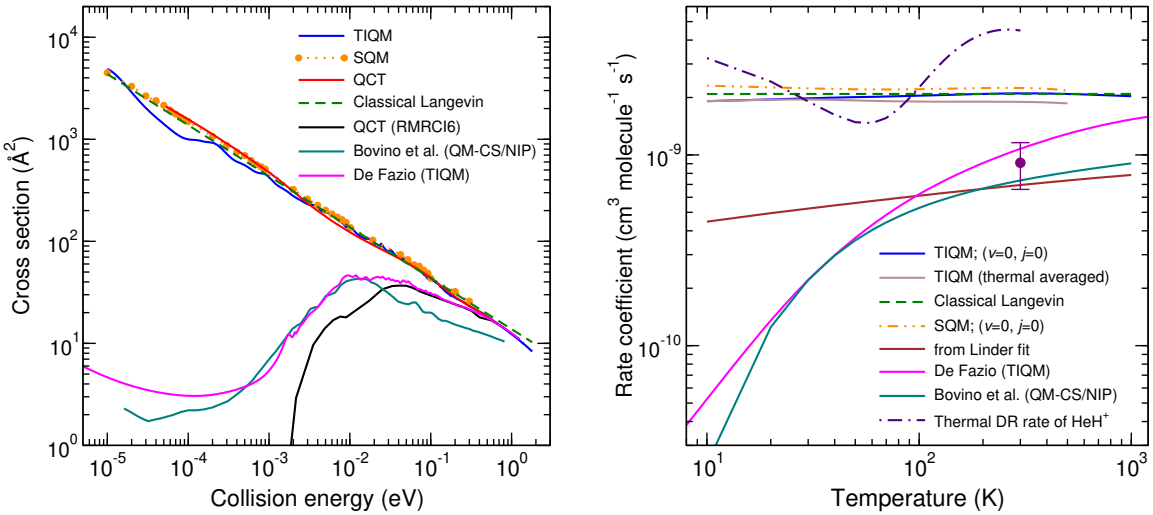

Figure 6: Left: Initial state-selected total ICS of reaction (R1) for HeH^+ (v=0, j=0) as a function of collision energy on the new refined PES calculated by TIQM, SQM and QCT methods. The ICS obtained by the classical Langevin model, QCT ICS of the present work on RMRCI6 PES, TIQM ICS of De Fazio[86] and QM-CS/NIP ICS of Bovino *et al.*[84] are also shown for comparison. **Right:** Initial state-selected and thermal rate coefficients of reaction (R1) calculated by TIQM and SQM methods on the new refined PES compared with those obtained from classical Langevin model, the Linder fit[115] of the cross section, the TIQM thermal rate coefficient of De Fazio[86], QM-CS/NIP rate coefficients of Bovino *et al.*[83] and the experimental result at T = 300 K by Karpas *et al.*[79] (purple circle with error bars). The experimental thermally averaged dissociative recombination rate of HeH^+ from Novotný *et al.*[68] is also shown for comparison.

the ICSs computed using the new "refined" PES and those using the RMRCI6 PES. The ICS computed by De Fazio[86] and Bovino *et al.*[83] show an abrupt decrease below 10 meV, whereas the present ICSs computed by three different methods, namely TIQM, SQM and QCT, continue to increase with further decrease in collision energy below 10 meV, and most importantly closely follow the ICS from classical Langevin model. The large quantitative disparity in the low energy cross sections (roughly 3 orders of magnitude at 10 μeV of collision energy) has translated into a substantial difference in the low temperature rate coefficients as shown in the right panel of Fig. 6. Here the initial state-selected and thermal rate coefficients of reaction (R1) calculated by TIQM method on the "refined" PES are compared with the previous experimental[79,115] and theoretical results[83,86] from RMRCI6 PES within a temperature range of 10-1000 K. The classical Langevin and SQM rate coefficients are also shown for comparison. It can be seen that the present TIQM rate coefficient for HeH^+ (v=0, j = 0) closely follows both the classical Langevin rate and the SQM prediction within 10-1000 K. The same can also be seen for the TIQM thermal rate, although it is slightly lower than the Langevin rate. The presence of so-called "artificial" barrier in the H +

HeH^+ threshold of RMRCI6 PES is responsible for the rapid decrease of rate coefficients of De Fazio[86] and Bovino *et al.*[83] below ~ 300 K. This results in roughly 2 orders of magnitude difference in the rate at $T \sim 10$ K. A steep positive temperature dependence of rate coefficient is very unusual for exoergic-barrierless reactions and commonly occurs in case of reactions with a barrier on the reaction path.[9] Such rapid decrease is not observed in the present case where the new "refined" PES is truly barrierless, thus producing an almost temperature-independent rate having a reasonably good agreement with the Langevin rate. Our study reveals that the reasonable agreement between the experimental data at 300 K from Karpas *et al.*[79] and the rate coefficient computed by De Fazio[86] was fortuitous since this previous calculation used a PES characterised by an incorrect behavior at low collisional energy due to the "artificial" entrance barrier. Moreover, the comparison of our new TIQM and SQM rate coefficients of reaction (R1) with the experimental thermal rate of dissociative recombination (DR) of HeH^+ from Ref. 68 indicates that the destruction of HeH^+ by H may become as significant as the DR process below 100 K. This challenges the previously held notion that the DR process is the predominant mechanism for the destruction of primordial HeH^+ at low redshifts.[83]

V. CONCLUSION

In summary, we demonstrate that the significant decrease in low energy ICS and low-temperature rate coefficient for the $H + HeH^+ \rightarrow H_2^+ + He$ reaction in previous theoretical calculations[83–89] was due to an "artificial" barrier near the entrance channel on the PES of Ramachandran *et al.*[78] By focusing on the attractive two-body long-range interaction potential, we removed this barrier and developed a new, refined barrierless global PES for the electronic ground state of the HeH_2^+ reactive system. This new PES closely matches newly calculated *ab initio* electronic energies. The resulting ICSs and rate coefficients, derived from various classical, quantum, and statistical methods, exhibit typical exoergic-barrierless ion-neutral reaction characteristics, influenced by ion-induced dipole long-range interactions. The new rate coefficient at around 10 K is about two orders of magnitude larger than previous values, emphasizing the importance of long-range interactions in PES construction. Future experimental studies and further exploration of rate coefficients across broader temperatures, including ultracold conditions, will be vital for validating our theoretical predictions and understanding long-range interactions in this reaction.

SUPPLEMENTARY MATERIAL

The supplementary material contains topographical details of electronic ground state PES of HeH_2^+, details of construction of new refined PES, computational details of the TIQM method and additional results. It contains also a fortran program of the refined PES.

ACKNOWLEDGEMENTS

This work has been supported by the Agence Nationale de la Recherche (ANR-HYTRAJ), Contract No. ANR-19-CE30-0039-01. Y.S. and J.S. thank support from the High Performance Computing Platform MESO@LR at the University of Montpellier. This work was also granted access to the HPC/AI resources of [CINES/IDRIS/TGCC] under the allocation 2023-2024 [AD010805116R2] made by GENCI. T.G.L. thnaks MCIN/AEI/10.130039/501100011033 PID2020-114654GB-I00 and 2024AEP119 support. Y.S thanks F. Lique for fruitful discussion.

AUTHOR DECLARATIONS

Conflict of Interest

The authors have no conflicts to disclose.

Author Contributions

Jayakrushna Sahoo: Conceptualization (equal); Data curation (equal); Formal analysis (equal); Funding acquisition (lead); Investigation (equal); Methodology (equal); Validation (equal); Visualization (equal); Writing – original draft (equal); Writing – review & editing (equal). **Duncan Bossion**: Conceptualization (equal); Data curation (equal); Formal analysis (equal); Funding acquisition (lead); Investigation (equal); Methodology (equal); Validation (equal); Visualization (equal); Writing – original draft (equal); Writing – review & editing (equal). **Tomás González-Lezana**: Conceptualization (equal); Data curation (equal); Formal analysis (equal); Validation (equal); Visualization (equal); Writing – original draft (equal); Writing – review & editing (equal). **Dahbia Tabi**: Conceptualization (equal); Data curation (equal); Formal analysis (equal); Funding acquisition (lead); Investigation (equal); Methodology (equal); Visualization

(equal); Writing – review & editing (equal). **Yohann Scribano**: Conceptualization (equal); Data curation (equal); Formal analysis (equal); Funding acquisition (lead); Investigation (equal); Methodology (equal); Project administration (lead); Resources (lead); Supervision (lead); Validation (equal); Visualization (equal); Writing – original draft (equal); Writing – review & editing (equal).

DATA AVAILABILITY

The data that support the findings of this study are available from the corresponding author upon reasonable request.

REFERENCES

[1]D. H. Zhang and H. Guo, Annu. Rev. Phys. Chem. **67**, 135 (2016).

[2]J. Li, B. Zhao, D. Xie, and H. Guo, J. Phys. Chem. Lett. **11**, 8844 (2020).

[3]D. J. Auerbach, J. C. Tully, and A. M. Wodtke, Nat Sci. **1**, e10005 (2021).

[4]H. Pan, B. Zhao, H. Guo, and K. Liu, J. Phys. Chem. Lett. **14**, 10412 (2023).

[5]M. Brouard and C. Vallance, *Tutorials in Molecular Reaction Dynamics*, RSC Publishing, UK, 2011.

[6]R. D. Levine, *Molecular Reaction Dynamics*, Cambridge University Press, New York, 2005.

[7]S. C. Althorpe and D. C. Clary, Annu. Rev. Phys. Chem. **54**, 493 (2003).

[8]D. C. Clary, Proceedings of the National Academy of Sciences **105**, 12649 (2008).

[9]D. C. Clary, Annu. Rev. Phys. Chem. **41**, 61 (1990).

[10]P. F. Weck and N. Balakrishnan, International Reviews in Physical Chemistry **25**, 283 (2006).

[11]D. Galli and F. Palla, Astron. Astrophys. **335**, 403 (1998).

[12]D. Galli and F. Palla, Annu. Rev. Astron. Astrophys. **51**, 163 (2013).

[13]E. Herbst and W. Klemperer, Astrophys. J. **185**, 505 (1973).

[14]A. G. G. M. Tielens, *The Physics and Chemistry of the Interstellar Medium*, Cambridge University Press, 2005.

[15]K. Lodders and B. Fegley, *Chemistry of Low Mass Substellar Objects*, pages 1–28, Springer Berlin Heidelberg, Berlin, Heidelberg, 2006.

[16]R. K. Janev, *Atomic and Molecular Processes in Fusion Edge Plasmas*, Springer New York, 1995.

[17]M. Capitelli et al., *Fundamental Aspects of Plasma Chemical Physics*, Springer Series on Atomic, Optical, and Plasma Physics, Springer New York, 2016.

[18]E. P. Wigner, Phys. Rev. **73**, 1002 (1948).

[19]H. R. Sadeghpour et al., Journal of Physics B: Atomic, Molecular and Optical Physics **33**, R93 (2000).

[20]A. Tsikritea, J. A. Diprose, T. P. Softley, and B. R. Heazlewood, J. Chem. Phys. **157**, 060901 (2022).

[21]I. W. M. Smith, Angewandte Chemie International Edition **45**, 2842 (2006).

[22]J. Marquette, B. Rowe, G. Dupeyrat, G. Poissant, and C. Rebrion, Chem. Phys. Lett. **122**, 431 (1985).

[23]W. H. Miller, J. Chem. Phys. **52**, 543 (1970).

[24]R. B. Bernstein, A. Dalgarno, H. Massey, and I. C. Percival, Proc. R. Soc. Lond. A **274**, 427 (1963).

[25]E. J. Rackham, T. González-Lezana, and D. E. Manolopoulos, J. Chem. Phys. **119**, 12895 (2003).

[26]E. J. Rackham, F. Huarte-Larranaga, and D. E. Manolopoulos, Chem. Phys. Lett. **343**, 356 (2001).

[27]T. González-Lezana, Int. Rev. Phys. Chem. **26**, 29 (2007).

[28]P. Pechukas and J. C. Light, J. Chem. Phys. **42**, 3281 (1965).

[29]P. Pechukas, J. C. Light, and C. Rankin, J. Chem. Phys. **44**, 794 (1966).

[30]J. C. Light, Discuss. Faraday Soc. **44**, 14 (1967).

[31]C. Seiler, S. D. Hogan, and F. Merkt, Phys. Chem. Chem. Phys. **13**, 19000 (2011).

[32]P. Allmendinger, J. Deiglmayr, J. A. Agner, H. Schmutz, and F. Merkt, Phys. Rev. A **90**, 043403 (2014).

[33]Y. Liu and K.-K. Ni, Annu. Rev. Phys. Chem. **73**, 73 (2022).

[34]T. P. Softley, Proc. R. Soc. A **479**, 20220806 (2023).

[35]A. B. Henson, S. Gersten, Y. Shagam, J. Narevicius, and E. Narevicius, Science **338**, 234 (2012).

[36]J. Jankunas, B. Bertsche, K. Jachymski, M. Hapka, and A. Osterwalder, J. Chem. Phys. **140**, 244302 (2014).

[37]P. Allmendinger et al., ChemPhysChem **17**, 3596 (2016).

[38]A. Klein et al., Nat. Phys. **13**, 35 (2017).

[39]S. D. S. Gordon et al., Nat. Chem. **10**, 1190–1195 (2018).

[40]J. Zou, S. D. S. Gordon, and A. Osterwalder, Phys. Rev. Lett. **123**, 133401 (2019).

[41]P. Allmendinger, J. Deiglmayr, K. Höveler, O. Schullian, and F. Merkt, J. Chem. Phys. **145**, 244316 (2016).

[42]E. I. Dashevskaya, I. Litvin, E. E. Nikitin, and J. Troe, J. Chem. Phys. **145**, 244315 (2016).

[43]J. D. Katharina Höveler and F. Merkt, Mol. Phys. **119**, e1954708 (2021).

[44]V. Zhelyazkova, F. B. V. Martins, J. A. Agner, H. Schmutz, and F. Merkt, Phys. Rev. Lett. **125**, 263401 (2020).

[45]F. B. V. Martins, V. Zhelyazkova, and F. Merkt, New J. Phys. **24**, 113003 (2022).

[46]V. Zhelyazkova, F. B. V. Martins, J. A. Agner, H. Schmutz, and F. Merkt, Phys. Chem. Chem. Phys. **23**, 21606 (2021).

[47]V. Zhelyazkova, F. B. V. Martins, M. Žeško, and F. Merkt, Phys. Chem. Chem. Phys. **24**, 2843 (2022).

[48]V. Zhelyazkova, F. B. V. Martins, and F. Merkt, Phys. Chem. Chem. Phys. **24**, 16360 (2022).

[49]V. Zhelyazkova, F. B. V. Martins, S. Schilling, and F. Merkt, J. Phys. Chem. A **127**, 1458 (2023).

[50]Y. Shagam et al., Nat. Chem. **7**, 921 (2015).

[51]E. Vogt and G. H. Wannier, Phys. Rev. **95**, 1190 (1954).

[52]K. Höveler et al., Phys. Rev. A **106**, 052806 (2022).

[53]M. Lara, P. G. Jambrina, F. J. Aoiz, and J.-M. Launay, J. Chem. Phys. **143**, 204305 (2015).

[54]A. D. Dörfler et al., Nat. Commun. **10**, 5429 (2019).

[55]J. Toscano, H. J. Lewandowski, and B. R. Heazlewood, Phys. Chem. Chem. Phys. **22**, 9180 (2020).

[56]A. Dalgarno, J. Phys. Conf. Ser. **4**, 10 (2005).

[57]S. Lepp and P. C. Stancil, *Molecular Astrophysics of Stars and Galaxies*, Clarendon Press, 1998.

[58]S. Lepp, P. C. Stancil, and A. Dalgarno, J. Phys. B: At. Mol. Opt. Phys. **35**, R57 (2002).

[59]S. Lepp and J. M. Shull, Astrophys. J. **280**, 465 (1984).

[60]R. Güsten et al., Nature **568**, 357 (2019).

[61]S. Lepp, Nat. Astron. **3**, 382 (2019).

[62]D. A. Neufeld et al., Astrophys. J. **894**, 37 (2020).

[63]J. M. Moorhead, R. P. Lowe, J. P. Maillard, W. H. Wehlau, and P. F. Bernath, Astrophys. J. **326**, 899 (1988).

[64]C. Cecchi-Pestellini and A. Dalgarno, Astrophys. J. **413**, 611 (1993).

[65]X.-W. Liu et al., Monthly Notices of the Royal Astronomical Society **290**, L71 (1997).

[66]H. L. Dinerstein and T. R. Geballe, Astrophys. J. **562**, 515 (2001).

[67]I. Zinchenko, V. Dubrovich, and C. Henkel, Monthly Notices of the Royal Astronomical Society: Letters **415**, L78 (2011).

[68]O. Novotný et al., Science **365**, 676 (2019).

[69]R. Čurík, D. Hvizdoš, and C. H. Greene, Phys. Rev. Lett. **124**, 043401 (2020).

[70]R. C. Forrey, J. F. Babb, E. D. S. Courtney, R. T. McArdle, and P. C. Stancil, Astrophys. J. **898**, 86 (2020).

[71]F. A. Gianturco et al., J. Chem. Phys. **154**, 054311 (2021).

[72]L. H. Scarlett, M. C. Zammit, I. Bray, B. I. Schneider, and D. V. Fursa, Phys. Rev. A **106**, 042818 (2022).

[73]K. Giri et al., J. Phys. Chem. A **126**, 2244 (2022).

[74]B. Desrousseaux and F. Lique, J. Chem. Phys. **152**, 074303 (2020).

[75]Y. Kulinich, B. Novosyadlyj, V. Shulga, and W. Han, Phys. Rev. D **101**, 083519 (2020).

[76]E. D. S. Courtney, R. C. Forrey, R. T. McArdle, P. C. Stancil, and J. F. Babb, Astrophys. J. **919**, 70 (2021).

[77]A. Faure, P. Hily-Blant, G. P. des Forêts, and D. R. Flower, Monthly Notices of the Royal Astronomical Society **531**, 340 (2024).

[78]C. N. Ramachandran, D. D. Fazio, S. Cavalli, F. Tarantelli, and V. Aquilanti, Chem. Phys. Lett. **469**, 26 (2009).

[79]Z. Karpas, V. Anicich, and J. Huntress, W. T., J. Chem. Phys. **70**, 2877 (1979).

[80]J. A. Rutherford and D. A. Vroom, J. Chem. Phys. **58**, 4076 (1973).

[81]J. Lv, X. Liu, J. Liang, and H. Sun, Can. J. Phys. **88**, 899 (2010).

[82]J. Liang, X. Liu, W. Xu, H. Kong, and Q. Zhang, Journal of Molecular Structure: THEOCHEM **942**, 93 (2010).

[83]S. Bovino, M. Tacconi, F. A. Gianturco, and D. Galli, Astron. Astrophys. **529**, A140 (2011).

[84]S. Bovino, M. Tacconi, and F. A. Gianturco, J. Phys. Chem. A **115**, 8197 (2011).

[85]S. Bovino, F. Gianturco, and M. Tacconi, Chem. Phys. Lett. **554**, 47 (2012).

[86]D. De Fazio, Phys. Chem. Chem. Phys. **16**, 11662 (2014).

[87]P. Gamallo, S. Akpinar, P. Defazio, and C. Petrongolo, J. Phys. Chem. A **118**, 6451 (2014).

[88]F. Esposito, C. M. Coppola, and D. De Fazio, J. Phys. Chem. A **119**, 12615 (2015).

[89]T. González-Lezana, D. Bossion, Y. Scribano, S. Bhowmick, and Y. V. Suleimanov, J. Phys. Chem. A **123**, 10480 (2019).

[90]H. Werner and P. J. Knowles, J. Chem. Phys. **89**, 5803 (1988).

[91]P. J. Knowles and H.-J. Werner, Chem. Phys. Lett. **145**, 514 (1988).

[92]P. Knowles and N. Handy, Chem. Phys. Lett. **111**, 315 (1984).

[93]P. J. Knowles and N. C. Handy, Comput. Phys. Commun. **54**, 75 (1989).

[94]J. Dunning, Thom H., J. Chem. Phys. **90**, 1007 (1989).

[95]A. Aguado and M. Paniagua, J. Chem. Phys. **96**, 1265 (1992).

[96]D. Koner, J. C. San Vicente Veliz, A. van der Avoird, and M. Meuwly, Phys. Chem. Chem. Phys. **21**, 24976 (2019).

[97]A. K. Wilson, T. van Mourik, and T. H. Dunning, Journal of Molecular Structure: THEOCHEM **388**, 339 (1996).

[98]D. E. Woon and J. Dunning, Thom H., The Journal of Chemical Physics **100**, 2975 (1994).

[99]M. F. Falcetta and P. E. Siska, Mol. Phys. **97**, 117 (1999).

[100]D. M. Bishop and J. Pipin, Chem. Phys. Lett. **236**, 15 (1995).

[101]H. Werner and W. Meyer, The Journal of Chemical Physics **73**, 2342 (1980).

[102]H. Werner and P. J. Knowles, The Journal of Chemical Physics **82**, 5053 (1985).

[103]H.-J. Werner et al., Molpro, version 2022.1, a package of ab initio programs, see https://www.molpro.net.

[104]D. Skouteris, J. Castillo, and D. Manolopoulos, Comput. Phys. Commun. **133**, 128 (2000).

[105]D. E. Manolopoulos, J. Chem. Phys. **85**, 6425 (1986).

[106]S. D. Chao et al., J. Chem. Phys. **117**, 8341 (2002).

[107]J. Z. H. Zhang and W. H. Miller, J. Chem. Phys. **91**, 1528 (1989).

[108]D. Bossion, S. Ndengué, H.-D. Meyer, F. Gatti, and Y. Scribano, J. Chem. Phys. **153**, 081102 (2020).

[109]D. G. Truhlar and J. T. Muckerman, *Reactive Scattering Cross Sections III: Quasiclassical and Semiclassical Methods*, pages 505–566, Springer US, Boston, MA, 1979.

[110]M. Karplus, R. N. Porter, and R. D. Sharma, J. Chem. Phys. **43**, 3259 (1965).

[111]M. V. Berry and K. E. Mount, Reports on Progress in Physics **35**, 315 (1972).

[112]M. Langevin, Une formule fondamentale de théorie cinétique, in *Annales de chimie et de physique, Series*, volume 5, pages 245–288, 1905.

[113]H. Eyring, J. O. Hirschfelder, and H. S. Taylor, J. Chem. Phys. **4**, 479 (1936).

[114]G. Gioumousis and D. P. Stevenson, J. Chem. Phys. **29**, 294 (1958).

[115]F. Linder, R. K. Janev, and J. Botero, *Reactive Ion-molecule Collisions Involving Hydrogen and Helium*, pages 397–431, Plenum Press, New York, 1995.